ARCHIVES OF ELECTRICAL ENGINEERING VOL. 67(4), pp. 815–828 (2018)

DOI 10.24425/aee.2018.124742

A new power management strategy for PV-FC-based autonomous DC microgrid

PRAMOD BHAT NEMPU, N. SABHAHIT JAYALAKSHMI

Department of Electrical and Electronics Engineering
Manipal Institute of Technology, Manipal Academy of Higher Education
Manipal, Udupi - 576104, India
e-mail: jayalakshmi.ns@manipal.edu

(Received: 02.02.2018, revised: 16.08.2018)

Abstract: Solar energy is widely available in nature and electricity can be easily extracted using solar PV cells. A fuel cell being reliable and environment friendly becomes a good choice for the backup so as to compensate for continuously varying solar irradiation. This paper presents simple control schemes for power management of the DC microgrid consisting of PV modules and fuel cell as energy sources and a hydrogen electrolyzer system for storing the excess power generated. The supercapacitor bank is used as a short term energy storage device for providing the energy buffer whenever sudden fluctuations occur in the input power and the load demand. A new power control strategy is developed for a hydrogen storage system. The performance of the system is assessed with and without the supercapacitor bank and the results are compared. A comparative study of the voltage regulation of the microgrid is presented with the controller of the supercapacitor bank, realized using a traditional PI controller and an intelligent fuzzy logic controller.

Key words: DC microgrid, electrolyzer, fuzzy logic controller, PEM fuel cell, PV Array, supercapacitor bank

1. Introduction

Due to high efficiency, direct current (DC) appliances are preferred everywhere. Also, renewable energy sources are being used for meeting the increased energy demand due to the fact that they are freely available in nature and are environmental friendly. Solar energy is generally used for generating electrical power as the solar PV modules have negligible maintenance cost. A fuel cell (FC) is the alternate energy source which produces DC power by consuming hydrogen. If the PV system output exceeds the demand, the surplus power is stored in a hydrogen tank using electrolyzer, so that the stored hydrogen can be used for power generation from the FC, whenever necessary. Since a supercapacitor (SC) is capable of charging and discharging faster, it is preferred for short time storage.

In [1], a comprehensive review of renewable energy gadgets is performed and the scope for mitigating harmful gases like CO_2 is provided. An in depth survey of present status and future possibilities of different renewable energy-based systems, power electronics control-based hybrid systems and their configuration is reported in [2]. The problem of climate change and the unpredictability of oil make the use of non-conventional fuel significant. In paper [3], authors have investigated the potential for solar, wind and biomass sources for delivering energy. Emphasis is given to land prospects and restrictions on cost of production as a function of availability of resources and innovation subtleties. The material properties and application details of TiO_2 nanotube arrays for solar energy applications are provided in [4]. The operating principle and various properties of different types of PV modules are described in [5]. The analysis of useful work or exergy in different solar systems such as heaters, desalination systems, refrigeration and power generation systems is given in [6]. In this work, PV is used as main energy source based on these literatures and considering the reliability as the major factor, fuel cell is used for backup.

The simulation and experimental study of a maximum power point tracking (MPPT) control technique for the photovoltaic array is described in [7]. In [8], a detailed simulation analysis of a PV array is provided. In paper [9], a PV array-based stand-alone power system with a battery is described and in [10] control strategies for a hybrid energy storage system involving a battery and SC is discussed for a PV-based stand-alone distributed generation (DG) system. The battery is regulated by a current-voltage control technique for energy balance and the SC bank is controlled by a V–I control technique for short-term energy management. The PV and proton exchange membrane fuel cell (PEMFC)-based stand-alone hybrid system is proposed with an ultracapacitor or supercapacitor as the only storage device in [11]. The authors used PV as it is available in abundance and extracting electricity from PV is easier. The PEMFC is chosen considering its high reliability. When the FC is used the SC bank is essential as the FC has slow dynamics. Paper [12] describes the PV and FC-based hybrid system with direct connection of the supercapacitor bank without controllers.

A decentralized PV, wind and FC-based independent microgrid with multiple generation systems are described in [13] and a comparison is performed with the centralized control scheme for validating its effectiveness in minimizing the net present cost. The same system is analyzed with a multi-agent decentralized energy management system (DEMS) with game theory. A comparative study with fuzzy cognitive maps (FCM) is provided in [14]. In [15], the feasibility of a microturbine and FC hybrid system with an electrolyzer is examined with fuzzy logic-based self-tuning controllers for frequency regulation. The paper [16] describes a PV powered desalination structure in a DC microgrid conception integrating a hybrid short-term energy storage using hybrid capacitors and a hydraulic energy storage. A multi-agent DEMS which employs an FCM for operation permitting helps in efficient operation of the system. In paper [17], an energy system model for evaluating energy storage systems in microgrids with improved algorithms is developed. An organized method for optimizing the size and life cycle for a hybrid energy storage system is developed using a direct algorithm in [18].

In [19], grid connected operation of a wind-solid oxide fuel cell hybrid system is described with a hydrogen electrolyzer and supercapacitor as storage devices. Wind and FC-based stand-alone hybrid systems with an electrolyzer-based hydrogen storage system are described in [20]. A similar system is studied with the PV as the main source in [21]. The PV and wind systems with fuel cells are described without a SC in [22]. In [23], an investigation of cost-effectiveness

of the hydrogen storage system is reported considering industrial loads. PEM electrolysis is an alternative for hydrogen generation from renewable sources. Certain applications like stand-alone and grid assisted hydrogen production, using an electrolyzer for peak shaving, etc. are discussed in [24]. The neural network-based online method for regulating the operation of PEMFC for residential application is detailed in [25]. In [26], stand-alone operation of the PV-FC hybrid system is described considering AC and DC loads with a battery as the energy storage device. Fuzzy logic controllers (FLCs) are used for voltage and frequency regulation, using an inverter. In [27], the SC-based power smoothing technique is described for grid connected operation of renewable energy sources. In [28], details of operation and design power electronic converters are provided. The fundamentals and application details of fuzzy logic controllers are provided in [29].

This paper proposes a new method with simpler control techniques for regulating the operation of a DC microgrid consisting of the PV-PEMFC hybrid system with a hydrogen storage system and SC bank. The control strategies are developed for the PEMFC and hydrogen storage, using single PI controllers to reduce complexity of the system. The comparative analysis of the microgrid operation with a V–I controlled FC stack without the SC bank and a current controlled FC stack with the V–I controlled SC bank is provided. A comparison of the voltage regulation of the system with a traditional PI controller and FLC in the outer loop of the SC bank controller is reported.

In this article, section 2 gives an overview of the autonomous DC microgrid. In section 3, a brief description about the modeling of sources and a storage system is provided. In section 4, various control techniques employed for regulating the operation of a microgrid are reported. In section 5 the simulation results are analyzed. The conclusions are made in section 6.

2. Configuration of microgrid

The schematic representation of the DC microgrid with a PV-PEMFC autonomous DC microgrid is shown in Fig. 1. In this system, the main power source is a PV array of 13.75 kW capacity; a PEMFC stack of capacity 10 kW serves as the backup source as maximum load expected on the system is considered as 12 kW. An electrolyzer is used to generate hydrogen based on the difference between load and generation when power generated from the PV array exceeds the load demand. A SC bank with a capacity of 250 V, 4 F is used for providing or absorbing power during sudden changes in demand and to simultaneously regulate DC bus voltage. The SC bank is designed based on the current required, FC start-up time and DC bus voltage deviation as given in [12]. The sources are coupled to the DC bus. The PV array consists of an incremental conductance MPPT algorithm along with a boost converter [11] for extracting the power corresponding to maximum power point. The MPPT controller uses a PI controller for reducing the error between the conductance $\left(\frac{I_{\mathrm{PV}}}{V_{\mathrm{PV}}}\right)$ and negative of incremental conductance $\left(\frac{\mathrm{d}\, I_{\mathrm{PV}}}{\mathrm{d}\, V_{\mathrm{PV}}}\right)$ by adjusting the duty ratio of the PV system's boost converter. The SC bank is regulated by a voltage-current (V–I) control strategy using a bidirectional DC–DC converter. The V–I control scheme maintains the DC bus voltage and compensates for power transients. The controller of the FC stack balances the power generation among the PV and PEMFC as per the load requirements when the load is more than the power generated from the PV array. A power controller is developed to store the surplus power generated in a hydrogen electrolyzer system using a buck converter.

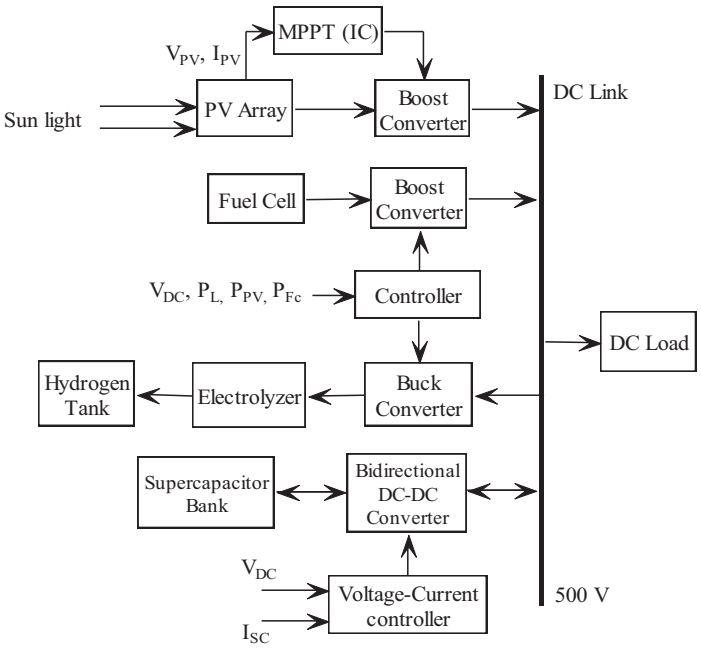

Fig. 1. Schematic diagram of the DC microgrid

3. Modeling of PV array, fuel cell and electrolyzer system

3.1. Modeling of PV array

Modeling of the PV array is described in [7, 8, 11]. The current produced in PV array I_{PV} is given in Equation (1).

$$I_{\mathrm{PV}} = N_p \times I_{ph} - N_p \times I_r \times \exp\left[\frac{q \times \left(N_p V_o + N_s I_o R_s\right)}{N_s N_p k T_c n} - 1\right], \tag{1}$$

where n is the cell idealizing factor, I_{ph} is the photovoltaic current, T_c is the absolute temperature of a solar cell (K), I_r is the reverse saturation current, q is the charge of a single electron, k is the Boltzmann's constant, N_s and N_p are, respectively, the number of cells in series and parallel, R_p and R_s are the shunt and series resistance of a solar cell, respectively (Ω), V_o is the terminal voltage of a solar cell and I_o is the output current of a solar cell.

3.2. Modeling of PEMFC stack and electrolyzer system

The output power of a PEMFC stack is given as a function of flow rate (q) and partial pressure (p) of H_2, O_2 and water [21]. The voltage output of the PEMFC is given by the sum of Nernst voltage and losses. Nernst instantaneous voltage is given by Equation (2).

$$E = N_o \times \left[E_0 + \frac{RT}{2F} \times \log\left(\frac{p_{\mathrm{H_2}} \times \sqrt{p_{\mathrm{O_2}}}}{p_{\mathrm{H_2O}}}\right)\right]. \tag{2}$$

E_o is the no load voltage (V), N_o is the number of cells in series, F is Faraday's constant (C/kmol), R_{int} is the fuel cell's internal resistance, R is the universal gas constant (8314.47 J/kmol · K), T is the absolute temperature of a FC and E is the Nernst instantaneous voltage. Modeling of an electrolyzer system and hydrogen tank is discussed in [20, 21].

$$\eta_{\mathrm{H}_2} = \frac{\eta_F n_C i_e}{2 \times F}, \tag{3}$$

$$\eta_F = 96.5 \times e^{(0.09/i_e - 75.5/i_e^2)}, \tag{4}$$

$$P_b - P_{b_i} = z \frac{N_{\mathrm{H}_2} R T_b}{M_{\mathrm{H}_2} V_b}. \tag{5}$$

η_{H_2} is the hydrogen produced per second (mol/s), F is the Faraday's constant (C/kmol), n_C is the number of cells of the electrolyzer in series, η_F is the Faraday efficiency and i_e is the electrolyzer current (A). P_b is the pressure of the tank (Pascal), P_{b_i} is the initial pressure (Pascal), M_{H_2} is the molar mass of hydrogen (kg kmol^{-1}), N_{H_2} is the hydrogen delivered to the tank (kmol/s), R is the Rydberg constant (J/kmol·K), T_b is the temperature (K), V_b is the volume of the tank (m^3) and z is the compressibility factor.

4. Control strategies for power management

In this section control strategies applied for a FC system, electrolyzer and supercapacitor bank for the power management of a microgrid are discussed in detail.

4.1. Controller of fuel cell system

Fig. 2(a) and Fig. 2(b) show the schematic of a current controller and V–I controller applied to the boost converter of a FC stack, respectively. The current controller is realized using a PI controller and a selection switch. The V–I controller has an outer loop to regulate voltage at a DC bus (V_{DC}) and an inner loop to control the FC current for balancing power. The V–I controller is used when a SC bank is removed from the system. The current controller is used when the VηI controlled SC bank is introduced into the system. When the load current (I_L) exceeds the current generated from the PV array (I_{PV}), the difference between demand and generation is met by the FC stack as per the control strategy. The deficit in the generation is compared with the current

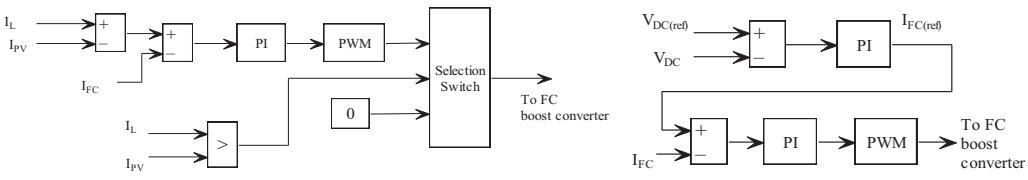

(a) (b)

Fig. 2. Fuel cell controller: current controller (when SC bank is used) (a); V–I controller (when SC bank is not used) (b)

output of the FC system (I_{FC}) and the PI regulator reduces the error generating an appropriate duty ratio making the FC generate current required to meet the load demand in a current control scheme.

4.2. Power control of electrolyzer system

Fig. 3 shows the schematic of the proposed power control strategy applied to the buck converter of an electrolyzer. It is also realized using a single PI controller and a selection switch. When the load demand (P_L) is less than the power generated from the PV array (P_{PV}), the excess in generation is fed as the reference power to the electrolyzer and using a PI controller electrolyzer is made to produce hydrogen according to the command from the controller. The produced hydrogen is stored in a hydrogen tank. The PI controller is used to make the difference between the reference signal ($P_{\mathrm{PV}} - P_L$) zero so that the feedback (P_{EL}) follows the reference. As the microgrid is highly dynamic in nature with fluctuations both on load and source side, it is hard to find a fixed mathematical model. Hence the PI controller is tuned by the trial-and-error method.

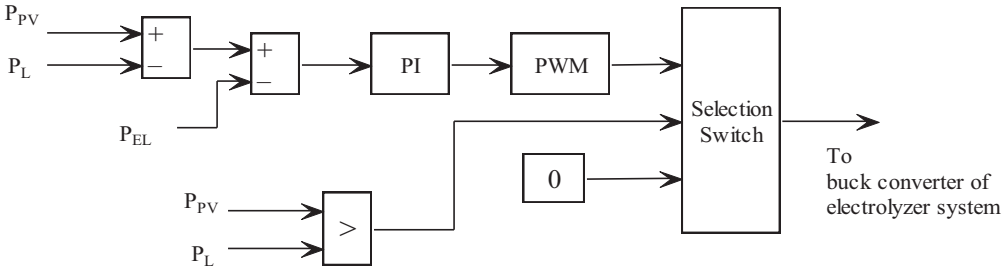

Fig. 3. Schematic diagram of electrolyzer controller

4.3. Voltage-current controller of supercapacitor bank

Fig. 4(a) and Fig. 4(b) show the schematic of the controller of the SC bank with a PI controller and FLC, respectively. During the fluctuations in the PV output and load demand, the FC fails to meet the demand quickly due to slow dynamics and hence a supercapacitor bank is used. The V–I control technique used for the SC bank helps to achieve quick power balance in the microgrid by absorbing or providing the power during sudden variations in the load. This control scheme regulates the DC link voltage. Based on the increase or decrease in voltage at a DC bus during power variations, the SC bank either charges or discharges. The current output of the SC bank is I_{SC}. To tune the PI controller, an auto-tuning method is used based on the transfer function of a bidirectional DC–DC converter [27] as in Equations (6) and (7).

$$G_{id}(s) = \frac{V_o\left(sC + \dfrac{2}{R}\right)}{s^2LC + s\dfrac{L}{R} + (1-D)^2}, \tag{6}$$

$$G_{vi}(s) = \frac{(1-D)\left[1 - \dfrac{sL}{R(1-D)^2}\right]}{sC + \dfrac{2}{R}}, \tag{7}$$

where V_o is the output voltage of the converter, C is the converter's output capacitance, L is the inductance, D is the duty ratio and R is the resistance representing the load.

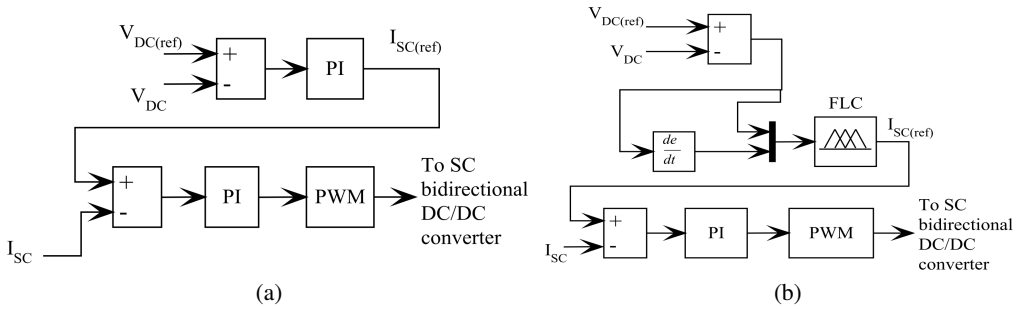

Fig. 4. Schematic of V–I controller of SC bank: with PI controller (a); with FLC (b)

Since constant voltage required for the operation of DC loads is regulated by this controller, the accuracy of voltage regulation is the major concern. Hence a FLC is applied to the outer loop of the V–I controller so as to observe the improvement in voltage regulation. The output of the FLC is the current reference for the SC bank. The FLC is realized using the fuzzy logic tool box of MATLAB. The FLC has two inputs. The first input is the error in DC bus voltage (e) and second one is change in error (Δe) which is the derivative of error i.e. $\dfrac{\mathrm{d}\,e}{\mathrm{d}\,t}$. The inputs are fuzzified using membership functions, fuzzified inputs produce a fuzzy output by the mamdani fuzzy inference scheme and the fuzzy output is a converter into crisp output by the centroid method of de-fuzzificaton. The input and output triangular membership functions are shown in Fig. 5.

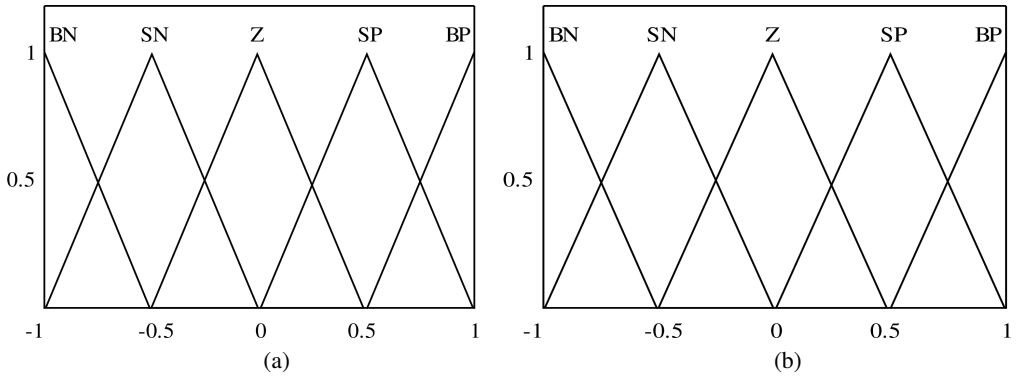

Fig. 5. Membership functions of FLC: inputs (a); output (b)

The rule base of the FLC [31] is shown in Table 1. Fuzzy sets are characterized as: Z is Zero, BN is Big Negative, SN is Negative Small, BP is Big Positive, SP is Small Positive. Example: If e is Big Positive and Δe is Small Negative, then the current reference is Big Positive.

Table 1. Rule base for FLC

$e/\Delta e$	**BN**	**SN**	**Z**	**SP**	**BP**
BN	BN	BN	BN	SN	Z
SN	BN	SN	SN	Z	SP
Z	BN	SN	Z	SP	BP
SP	SN	Z	SP	SP	BP
BP	Z	BP	BP	BP	BP

5. Results and discussions

Based on 24 hours irradiance data collected from [30], input to the solar PV array is provided from the signal builder block of Simulink from sun rise to sun set by scaling down the time axis to 7 seconds. Since the objective of the work is to validate the control techniques, for the ease of analysis, short time duration is considered. In order to simulate the system for 24 hours, the rating of the storage device employed should be accordingly increased. The input irradiance pattern is shown in Fig. 6(a). Based on the input of the PV array, the power output of the PV system is shown in Fig. 6(b). The output of the PV array is directly dependent on the input irradiance.

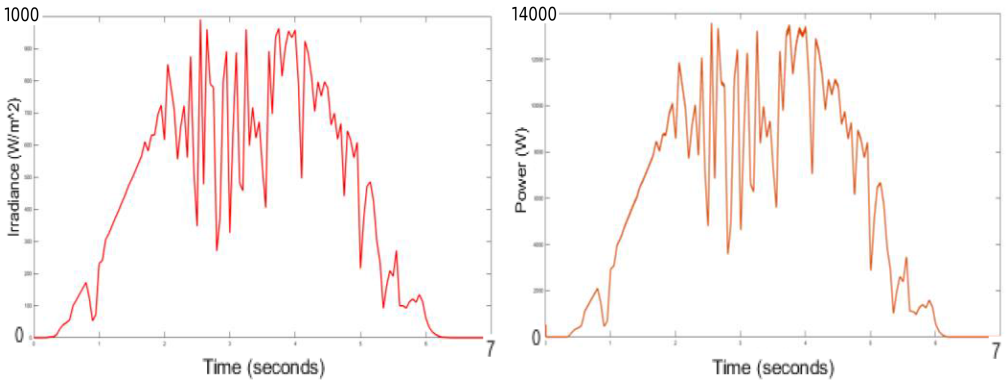

(a) (b)

Fig. 6. Irradiance input to the PV array and PV system output: irradiance input (a); power output of PV system (b)

Fig. 7 shows the power generated from all the sources, electrolyzer power and load demand. When the PV output exceeds the load power, surplus power is used to produce hydrogen which

is stored in a storage tank and when the demand exceeds the PV output power, the FC system supplies additional power required. The SC bank provides or absorbs power during sudden power fluctuations and helps in quick power balancing.

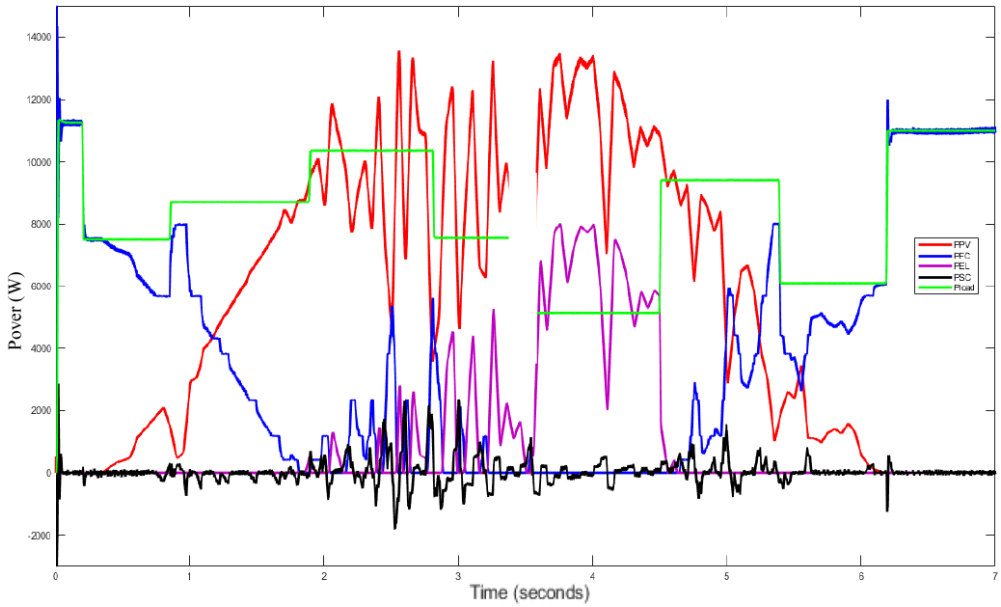

Fig. 7. Power generated, power stored and the load demand

The amount of hydrogen produced is shown in Fig. 8(a). Based on the power controller developed, a buck converter regulates the amount of power which has to be produced, so as to

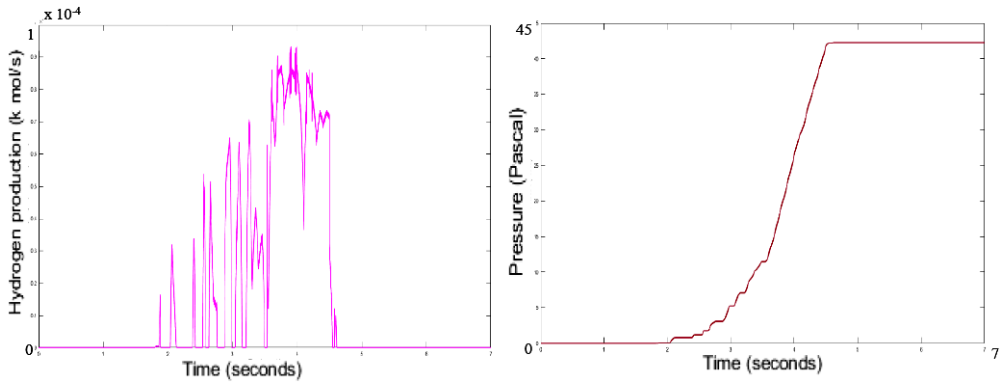

(a) (b)

Fig. 8. Hydrogen moles produced by electrolyzer and pressure of hydrogen tank: hydrogen moles produced (a); pressure of hydrogen tank (b)

generate hydrogen. The hydrogen generated is then sent to the storage tank. The pressure of the hydrogen tank is shown in Fig. 8(b).

Fig. 9 shows the total power supplied to the load and the load demand with and without the SC bank. High fluctuations are observed when the SC bank is absent and the V–I controlled FC stack is used for voltage and power regulation. It can be observed that under suddenly varying load conditions and highly intermittent source power, smooth power is supplied to the load when the current controlled FC and V–I controlled SC bank are employed in the system. The SC bank plays a significant role in providing smooth power to load due to its ability to charge and discharge quickly.

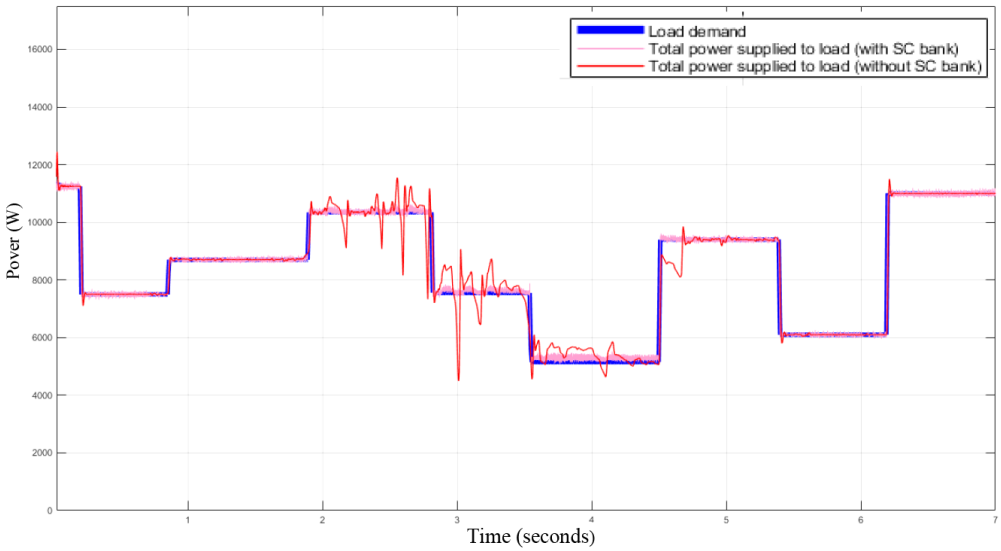

Fig. 9. Power demand and generation

Fig. 10 shows the Bode plot of the V–I controller of the SC bank when the PI controllers are tuned by an auto-tuning method. Controllers of outer and inner control loops are separately tuned and the closed loop stability is verified. The system is found to be stable as the phase margin and gain margin are positive.

Fig. 11 shows the regulated DC link voltage with and without the SC bank. The system voltage regulation is significantly improved when the controlled SC bank is used in the system. Due to slower dynamics, the PEMFC stack fails to regulate the voltage at a DC bus under highly intermittent conditions. Maximum fluctuation of 21 percent is observed without the SC bank.

In Fig. 12(a), it can be observed that the power fluctuations in the SC bank are less when controlled using the FLC in the outer loop as the current reference for the SC bank is generated from it. Fig. 12(b) shows the state of charge (SOC) of the SC bank, which varies as per its charge and discharge operation. The SC bank is designed so as to compensate for sudden variations in the system and since its duration of charging or discharging is smaller, variations in the SOC are minimal.

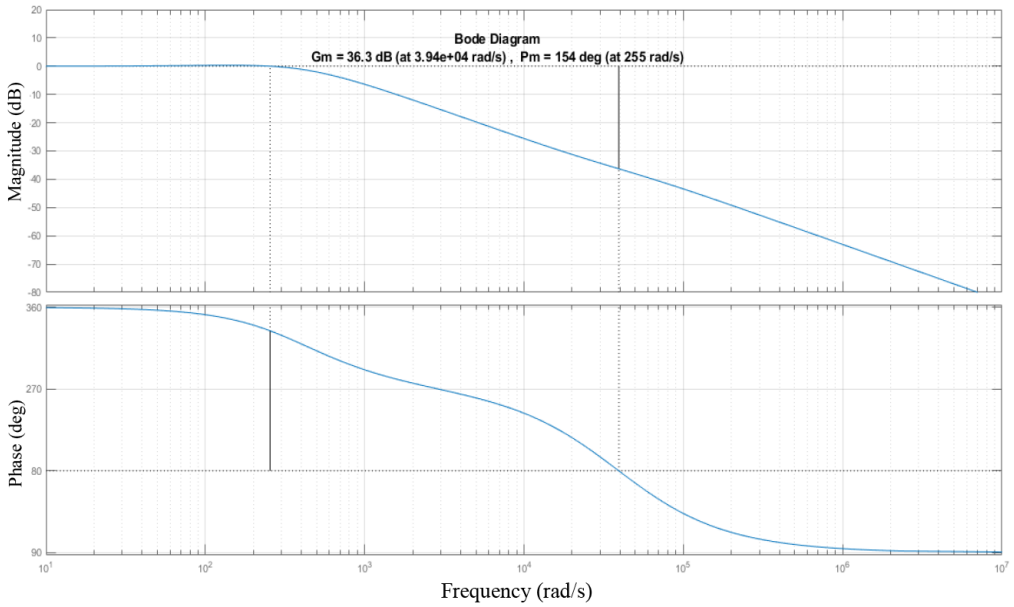

Fig. 10. Bode plot of SC bank control system

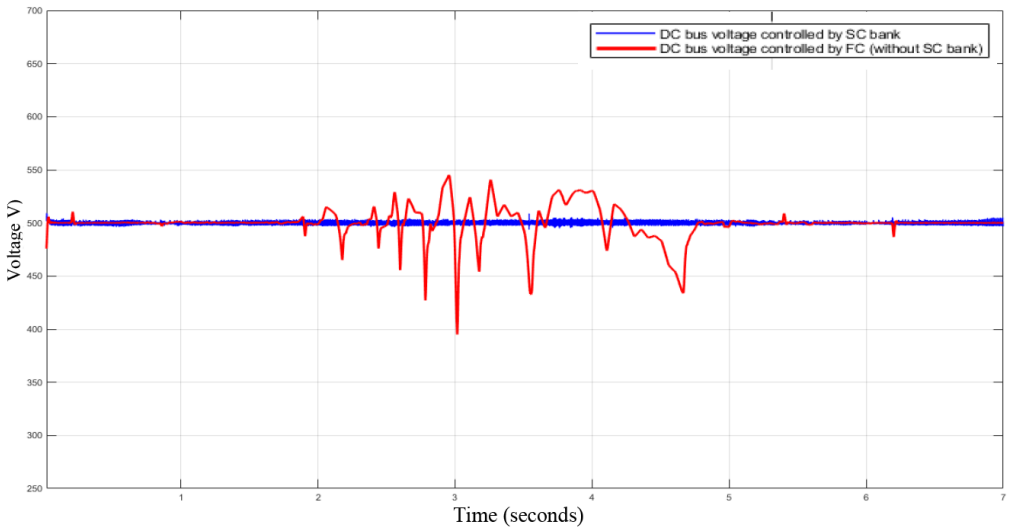

Fig. 11. DC link voltage with and without SC bank

Table 2 shows the parameters of the response with the PI controller and FLC. Overshoot is much less when the FLC is used instead of the PI controller and fluctuations in the voltage are less under varying source and load powers with the FLC-based V–I controller.

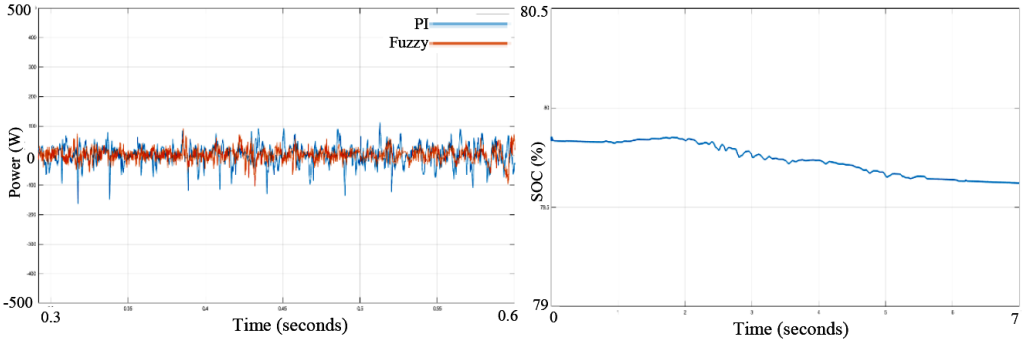

(a) (b)

Fig. 12. Supercapacitor power and SOC: SC bank power with PI controller and FLC (a); SOC of SC bank (b)

Table 2. Comparison of response of DC bus voltage obtained from PI controller and FLC

Parameter	PI controller	FLC
Overshoot (%)	6	< 1
Settling time (s)	0.01	0.02
Fluctuations	High	Low

6. Conclusions

In this work, dynamic models of the photovoltaic array, PEMFC stack and electrolyzer system are realized in MATLAB/Simulink. An incremental conductance-based MPPT algorithm is realized for a PV array. A current control strategy is realized for an FC stack for balancing power of the DC microgrid system based on load requirements. A new power control scheme is proposed for storing the surplus power generated by the PV array in a hydrogen storage system. A voltage-current controller is used to a control supercapacitor bank to manage power transients and DC link voltage regulation. The operation of the DC microgrid is analyzed with a V–I controlled FC stack without a SC bank and a current controlled FC stack with a V–I controlled SC bank and the results are compared. Improved performance in voltage regulation and power management is observed when the current controlled FC and V–I controlled SC bank are incorporated in the system. A comparative study of voltage regulation in the DC microgrid is performed using a PI controller and FLC in the outer loop of the V–I control strategy. The FLC shows better performance compared to the PI controller-based V–I controller. Thus a control scheme for effective power management and voltage regulation of the DC microgrid with the PV-PEMFC-SC hybrid system is developed. Future work will focus on employing advanced soft computing techniques for improving the operation of the DC microgrid.

References

[1] Panwar N.L., Kaushik S.C., Kothari S., *Role of renewable energy sources in environmental protection: a review*, Renewable and Sustainable Energy Reviews, vol. 15, no. 3, pp. 1513–1524 (2011).

[2] Ellabban O., Abu-Rub H., Blaabjerg F., *Renewable energy resources: Current status, future prospects and their enabling technology*, Renewable and Sustainable Energy Reviews, vol. 39, pp. 748–764 (2014).

[3] De Vries B.J.M., Van Vuuren D.P., Hoogwijk M.M., *Renewable energy sources: Their global potential for the first-half of the 21st century at a global level: An integrated approach*, Energy policy, vol. 35, no. 4, pp. 2590–2610 (2007).

[4] Mor G.K., Varghese O.K., Paulose M., Shankar K., Grimes C.A., *A review on highly ordered, vertically oriented TiO2 nanotube arrays: Fabrication, material properties, and solar energy applications*, Solar Energy Materials and Solar Cells, vol. 90, no. 14, pp. 2011–2075 (2006).

[5] Reinders A., Verlinden P., Freundlich A., *Photovoltaic solar energy: from fundamentals to applications*, John Wiley & Sons (2017).

[6] Saidur R., BoroumandJazi G., Mekhlif S., Jameel M., *Exergy analysis of solar energy applications*, Renewable and Sustainable Energy Reviews, vol. 16, no. 1, pp. 350–356 (2012).

[7] Natsheh E.M., Albarbar A., *Photovoltaic Model with MPP Tracker for Standalone/Grid Connected Applications*, IET Conference on Renewable Power Generation (RPG), Edinburgh, UK, pp. 1–6 (2011).

[8] Krishan R., Sood Y.R., Uday Kumar B., *The simulation and design for analysis of photovoltaic system based on MATLAB*, Int. Conf. Energy Efficient Technologies for Sustainability (ICEETS), Nagercoil, India, pp. 647–651 (2013).

[9] Jayalakshmi N.S., Gaonkar D.N., Balan A., Patil P., Raza S.A., *Dynamic Modeling and Performance Analysis of Stand-alone Photovoltaic System with Battery Supplying Dynamic Load*, International Journal of Renewable Energy Research, vol. 4, no. 3, pp. 635–640 (2014).

[10] Liu X., Wang P., Loh P.C., Gao F., Choo F.H., *Control of hybrid battery/ultracapacitor energy storage for stand-alone photovoltaic system*, IEEE Energy Conversion Congress and Exposition (ECCE), Atlanta, GA, USA, pp. 336–341 (2010).

[11] Jayalakshmi N.S., Gaonkar D.N., Nempu P.B., *Integrated Power Flow and Voltage Regulation of Stand-alone PV-Fuel cell System with Supercapacitors*, International Journal of Power and Energy Systems, vol. 37, no.1, pp. 1–9 (2017).

[12] Coelho R.F., Schimtz L., Martins D.C., *Grid Connected PV -Wind-Fuel Cell Hybrid System Employing a Supercapacitor Bank as Storage Device to Supply a Critical DC Load*, IEEE 33rd International Telecommunications Energy Conference, Amsterdam, Netherlands, pp. 1–10 (2011).

[13] Karavas C.S., Kyriakarakos G., Arvanitis K.G., Papadakis G., *A multi-agent decentralized energy management system based on distributed intelligence for the design and control of autonomous poly-generation microgrids*, Energy Conversion and Management, vol. 103, pp. 166–179 (2015).

[14] Karavas C.S., Kyriakarakos G., Arvanitis K.G., Papadakis G., *A Game Theory Approach to Multi-Agent Decentralized Energy Management of Autonomous Polygeneration Microgrids*, Energies, vol. 10, no. 11, p. 1756 (2017).

[15] Li X., Song Y.-J., Han S.-B., *Frequency control in micro-grid power system combined with electrolyzer system and fuzzy PI controller*, Journal of Power Sources, vol. 180, no. 1, pp. 468–475 (2008).

[16] Karavas C.S., Arvanitis K.G., Kyriakarakos G., Piromalis D.D., Papadakis G., *A novel autonomous PV powered desalination system based on a DC microgrid concept incorporating short-term energy storage*, Solar Energy, vol. 159, pp. 947–961(2018).

[17] Hittinger E., Wiley T., Kluza J., Whitacre J., *Evaluating the value of batteries in microgrid electricity systems using an improved Energy Systems Model*, Energy Conversion and Management, vol. 89, pp. 458–472 (2015).

[18] Shen J., Dusmez S., Khaligh A., *Optimization of sizing and battery cycle life in battery/ultracapacitor hybrid energy storage systems for electric vehicle applications*, IEEE Transactions on industrial informatics, vol. 10, no. 4, pp. 2112–2121 (2014).

[19] Ayyappa S.K., Gaonkar D.N., *Performance Analysis of a Variable-speed Wind and Fuel Cell Based Hybrid Distributed Generation System in Grid-connected Mode of Operation*, Electric Power Components and Systems, vol. 44, no. 2, pp. 1–10 (2016).

[20] Onar O.C., Uzunoglu M., Alam M.S., *Dynamic Modeling, Design and Simulation of a Wind/Fuel cell/Ultra-capacitor Based Hybrid Power Generation System*, Journal of Power Sources, vol. 161, no. 1, pp. 707–722 (2006).

[21] Uzunoglu M., Onar O.C., Alam M.S., *Modeling, control and simulation of a PV/FC/UC based hybrid power generation system for stand-alone applications*, Renewable Energy, vol. 34, pp. 509–520 (2009).

[22] Wang C., Nehrir M.H., *Power Management of a Stand-Alone Wind/Photovoltaic/Fuel cell Energy System*, IEEE Transactions on Energy Conversion, vol. 23, no. 3, pp. 957–967 (2008).

[23] Arlt M.L., Gonçalo Ferreira Cardoso, Weng D., *Hydrogen storage applications in industrial microgrids*, IEEE Green Energy and Smart Systems Conference (IGESSC), pp. 1–6, Long Beach, CA, USA (2017).

[24] Barbir F., *PEM electrolysis for production of hydrogen from renewable energy sources*, Solar energy, vol. 78, no. 5, pp. 661–669 (2005).

[25] Azmy A.M., Erlich I., *Online optimal management of PEM Fuel cells using neural networks*, IEEE Transactions on Power Delivery, vol. 20, no. 2, pp. 1051–1058 (2005).

[26] Vigneysh T., Kumarappan N., *Autonomous Operation and Control of Photovoltaic/Solid Oxide Fuel Cell/Battery Energy Storage Based Microgrid Using Fuzzy Logic Controller*, International Journal of Hydrogen Energy, vol. 41, no. 3, pp. 1–15 (2016).

[27] Somayajula D., Crow M., *An Ultracapacitor Integrated Power Conditioner for Intermittency Smoothing and Improving Power Quality of Distribution Grid*, IEEE Trans. Sustainable Energy, vol. 5, no. 4, pp. 1145–1155 (2014).

[28] Hart D.W., *Power Electronics*, Tata McGraw Hill Edition (2011).

[29] Ross T.J., *Fuzzy Logic with Engineering Applications*, John Wiley and Sons Inc., UK (2017).

[30] http://www.nrel.gov/midc/oahuarchive/ (data source from the National Renewable Energy Laboratory), accessed August 2014.

[31] Pati S., Mohanty K.B., Kar S.K., Mishra S., *Voltage and Frequency Control of a Micro-grid using a Fuzzy Logic Controller based STATCOM equipped with Battery Energy Storage System*, International Conference on Circuit, Power and Computing Technologies, Nagercoil, India, pp. 1–7 (2016).